

1 **Photocatalytic diphenhydramine degradation under different radiation sources:**
2 **kinetics studies and energetic comparison**

3
4 N. López, P. Marco, J.Giménez*, S.Esplugas
5 Department of Chemical Engineering and Analytical Chemistry, Faculty of Chemistry,
6 Universitat de Barcelona, C/Martí i Franqués 1, 08028 - Barcelona, Spain.Tel:
7 +34934020154. Fax: +34934021291

8 *Corresponding Author: j.gimenez.fa@ub.edu

9
10 **ABSTRACT**

11 The degradation of diphenhydramine hydrochloride (DPH)by TiO₂photocatalysiswas
12 studied under different radiation sources: UVC, black blue lamps (BLB), simulated solar
13 radiation (SB, Solarbox) and solar radiation (CPCs, Compound Parabolic Concentrators)
14 at lab and pilot plant scales. Results indicated that photolysis showed an important role
15 in the DPH abatement under UVC radiation (32.5% of DPH conversion), being negligible
16 in all other cases. Different TiO₂ concentrations (0.05, 0.1 and 0.4 g/L) were used in SB
17 device and the best results were obtained for 0.4 g/L:35.7% of DPH conversion,after 60
18 min of irradiation. For comparison purposes, concentration of 0.4 g/L TiO₂ were used in
19 all the devices. The best results obtained after 60 minutes of irradiation using only TiO₂
20 were 44.8% of DPH degradation in BLB and 9.0% of mineralization in SB. The addition
21 of H₂O₂ improves the photocatalytic process (without H₂O₂) and the best results obtained
22 were when UVC was used obtaining 100% DPH degradation and 28.6% TOC reduction.
23 Concerning the removal efficiencies to the energy used, the best results were obtained for
24 UVC with H₂O₂ (4492 mg DPH/kWh and 2246 ppm DPH/kWh), being also the
25 corresponding cheapest costs (2.89x10⁻⁵ €/mg DPH and 5.79x10⁻⁵ €/ppm DPH). In terms
26 of efficiency between 380-400 nm (absorption range for TiO₂), BLB presents the best
27 results. Kinetic constants were also estimated referred to the irradiation time (h⁻¹) or the
28 accumulated energy (kJ⁻¹), the highest values correspond to UVC with hydrogen peroxide
29 (7.64 h⁻¹ and 0.493 kJ⁻¹).Finally, toxicity and reaction intermediates were identified and
30 DPH photo-degradation pathway was proposed.

31 **KEYWORDS**

32 Diphenhydramine hydrochloride, simulated solar radiation, blacklight blue lamps, UVC,
33 CPC.

34 1. INTRODUCTION

35 In the last years, water scarcity and quality have become a worldwide concern [1]. Every
36 day large amounts of water are contaminated by different pollutants coming from
37 domestic or industrial uses. Pollution of water, regulated by Directive (2013/39/EU) [2]
38 as regards priority substances in the field of water policy, is generally decreasing.
39 However, organic substances with harmful properties such as pharmaceuticals and
40 personal care products are increasingly detected in the environment [3,4]. Spain is ranked
41 as one of the world's largest consumer of pharmaceuticals [5]. These compounds are
42 recalcitrant and with bioaccumulation problems [6, 7, 8]. They are also resistant to
43 conventional wastewater treatments and are found in effluents at concentrations ranging
44 0.1–20.0 µg/L [9,10,11].

45 Among those pollutants, there is a special group of pharmaceuticals, antihistaminic drugs,
46 easily found in waters. Between them, diphenhydramine hydrochloride (DPH) is the
47 classic H₁ receptor antagonist used in pregnancy for the treatment of allergies and nausea,
48 as well as an analgesic adjuvant in cancer pain. This kind of drugs can be achieved in
49 wastewaters coming from some pharmaceutical industries in concentrations between
50 1,300-1,400 µg/L and some antibiotics can reach concentrations between 28,000-31,000
51 µg/L [12]. DPH has relatively low molecular weight and high lipid solubility, allowing
52 easy blood–brain barrier and placental passage [13]. Unfortunately, information on the
53 environmental fate and toxicity to aquatic species is scarce for most pharmaceuticals [14].
54 Due to the growing demand of society for the decontamination of water, regulations are
55 increasingly strict in recent years, raising the research on methods to eliminate
56 pharmaceuticals from water and wastewater, and this is the case of advanced oxidation
57 processes (AOPs) [15,16].

58 AOPs are environmental friendly methods based on in situ production of hydroxyl radical
59 (\bullet OH) as main oxidant, which is able to react non-selectively with most organic
60 compounds [17]. Different studies have been reported related to the photocatalytic
61 treatment of DPH [18,19]. However, studies about DPH removal under different radiation
62 sources and at low catalyst concentrations have not yet been reported.

63 The present work is focused on the degradation and mineralization of DPH by
64 photocatalytic treatment in different experimental devices. Experiments were performed
65 in three laboratory scale photoreactors under artificial irradiation sources: UVC lamps

66 (monochromatic radiation, maximum at 254 nm), black blue lamps (emission ranging
67 from 300 to 410 nm, maximum at 365 nm) and simulated solar radiation (Solarbox with
68 Xe lamp, spectrum similar to the solar one in the UV range). Moreover, a solar reactor
69 has been used, at pilot plant scale, based on CPC configuration capable to collect the
70 direct and diffuse radiation [20]. The energetic and economic efficiencies of the different
71 tested devices were evaluated and compared. The most important intermediates have been
72 also proposed.

73 **2. MATERIALS AND EXPERIMENTAL SET-UPS**

74 **2.1. Chemicals and reagents**

75 The solution of 50 mg/L of DPH ($C_{17}H_{21}NO \cdot HCl$, HPLC grade, purity $\geq 98\%$ from
76 Sigma-Aldrich) was prepared using deionized water. This high concentration (50 mg/L)
77 was selected to assure accurate measurements of concentrations and to follow
78 TOC. Moreover, this concentration was chosen to represent the conditions of wastewater
79 coming from some pharmaceutical industries [21]. Acetonitrile (analytical reagent grade
80 from Fischer Chemical) and orthophosphoric acid (85% from PanreacQuimica) were used
81 for HPLC analysis. H_2O_2 (30% w/w, from Merck), $NaHSO_3$ and MeOH (PAI from
82 Panreac) reagents were used without further purification. Heterogeneous photocatalysis
83 was performed using TiO_2 P-25 (Evonik, Germany).

84 **2.2. Techniques and analytical instruments**

85 DPH concentration was monitored by HPLC from Waters using a SEA18 Teknokroma
86 column (250 x 4.6 mm i.d.; 5 μ m particle size) and a Waters 996 photodiode array
87 detector. The mobile phase was composed by water (pH 3) and acetonitrile (70:30),
88 injected with a flow-rate of 0.85 mL/min. DPH concentration was followed at UV
89 maximum absorbance (220 nm). TOC was analyzed with a Shimadzu TOC-V CNS
90 analyzer. H_2O_2 consumption was followed using the metavanadate spectrophotometric
91 method at 450 nm [22]. H_2O_2 contained in samples was quenched with sodium hydrogen
92 sulfite or the same volume of methanol, to avoid further reactions depending on the
93 analysis to be done. For the intermediates identification, samples were analyzed by the
94 electrospray ionization/mass spectrometry using an electrospray (ion spray) ESI-MS and
95 a LC/MSD-TOF (Agilent Technologies) mass spectrometer. With the purpose to evaluate
96 the acute toxicity depending of the different conditions Microtox[®] bioassays were

97 performed. This method measures the inhibition of light emission of bioluminescent
98 bacteria *vibrio fischeri* caused by the presence of toxic compounds in the aqueous media.
99 All the tests were carried out in a Microtox® M500 toxicity analyzer (Modern Water,
100 UK). All samples were filtered with a polyethersulfone membrane filter (0.45 µm,
101 Chemlab) to remove the catalyst before analytical procedures.

102 **2.3. Experimental devices**

103 All the experimental devices described below have already been used in other
104 investigations of the group and extensively described in other publications [23-25].

105 **2.3.1. Artificial irradiation: UVC reactor**

106 The experiments with UVC lamps were performed in a thermostatic Pyrex-jacketed 2 L
107 vessel (inner diameter 11 cm, height 23 cm), equipped with three low pressure mercury
108 lamps (Phillips TUV 8W, G8T5) located at the center of reactor. Lamps emit
109 monochromatic radiation (254 nm). The effective radiation power was measured by
110 ferrioxalate actinometry [26] and the obtained value was 4.31 J/s at 254 nm. A solution
111 of DPH (50 mg/L) was introduced in the reactor with TiO₂ (0.4 g/L), and immediately the
112 lamps were switched on. Next H₂O₂ (15, 75 or 150 mg/L) was added depending on the
113 experiment to be carried out. Magnetic stirring was used to ensure a good mixing. The
114 temperature of the solution was maintained constant at 25 °C with the recirculated water
115 by the jacket connected to an ultra-thermostatic bath (P Selecta).

116 **2.3.2. Artificial irradiation: Black Blue Lamps (BLB) reactor**

117 BLB reactor consists on a 2 L Pyrex-jacketed thermostatic vessel (inner diameter 11 cm,
118 height 23 cm), equipped with three 8W BLB lamps (Philips TL 8W-08 FAM) located at
119 the center of reactor. The radiative power was 1.55 J/s between 300-410 nm, measured
120 by o-nitrobenzaldehyde actinometry [22]. The used actinometry changes according to the
121 wavelength range of lamp emission. The tank was fed with DPH solution (50 mg/L) and
122 TiO₂ (0.4 g/L). H₂O₂ (15, 75 or 150 mg/L) was added depending on the experiment to be
123 carried out. The solution was maintained at constant temperature (25 °C) by controlling
124 the jacket temperature with an ultra-thermostatic bath (P Selecta).

125 **2.3.3. Artificial solar irradiation: Solarbox (SB)**

126 A Solarbox (CO.FO.ME.GRA, 220V, 50 Hz) was used with a Xenon lamp (Phillips
127 1kW), located at the top of the device. The effective radiation power was 0.97 J/s between
128 300-410 nm, measured also by o-nitrobenzaldehyde actinometry [22]. The tubular
129 photoreactor (24cm length, 2.11cm diameter, Duran glass material) was placed at the
130 bottom of the Solarbox on the axis of a parabolic mirror made of reflective aluminum. A
131 filter cutting off wavelengths under 280 nm was placed between the lamp and the reactor.
132 The DPH solution (50 mg/L) was prepared in a batch jacketed feeding tank (total volume
133 1L), connected to an ultra-thermostatic bath (Haake K10) to assure constant temperature
134 during the process. H₂O₂ (15, 75 or 150 mg/L) and TiO₂ (0.05, 0.1, 0.4 g/L) were added
135 depending on the experiment to be carried out. The solution to be treated was pumped to
136 solarbox by a peristaltic pump (Ecoline VC-280 II, Ismatec) from the feeding tank with
137 a flow-rate of 0.71 L/min. All connections employed were made of Teflon to avoid losses.
138 A preliminary sample was collected before irradiation, representing initial concentration
139 at time 0.

140 **2.3.4. Solar irradiation: CPC reactor**

141 Photocatalytic experiments were also carried out in a solar pilot plant based on compound
142 parabolic collectors (CPC), at the University of Barcelona (latitude 41.4 N, longitude
143 2.1W). The CPC consists in a module, 41° inclined, with a mirror made of polished
144 aluminum, with 6 parallel tubular quartz reactors (length 56 cm, inner diameter 1.75 cm,
145 wall thickness 0.15 cm). The total volume irradiated was 0.95 L. The total mirror's area
146 for solar irradiation capture-reflection was 0.228 m². Experiments were done between
147 12:00 and 18:00 hours in summer and temperature was 30 ± 5 °C. The exposure time was
148 enough to reach the total hydrogen peroxide consumption. The aqueous suspension of
149 DPH was pumped, with a peristaltic pump with a flow-rate 2.6 L/min, from the stirred
150 (RW 16 basic agitator IKA) reservoir tank (5 L) to irradiated quartz tubes and
151 continuously recirculated. The specific solar radiation was measured in each sample time
152 ranging 12.45 W/m² to 49.78 W/m², by a spectroradiometer Bentham DMc300. The
153 reservoir tank was fed with DPH solution (50 mg/L) and 0.4 g/L of TiO₂, with or without
154 H₂O₂ (0 or 150 mg/L).

155

156

157 3. RESULTS AND DISCUSSIONS

158 DPH degradation by photocatalysis was evaluated during one hour based on previous
159 experiments performed, in each experimental device. Different concentrations of H₂O₂
160 (15, 75 and 150 mg/L) and TiO₂ (0.05, 0.1 and 0.4g/L) were used depending on the
161 experiment to be carried out. These TiO₂ and H₂O₂ concentrations can be broadly found
162 in literature and they were also selected based on the previous experience [27,28,29,30].

163 In this section, degradation and mineralization results are shown with respect to the
164 accumulated energy (Q_{acc}, kJ/L), which was calculated according (Eq. 1) [22,31].

$$165 \quad Q_{acc} = \sum_{i=0}^n \frac{I \cdot \Delta t_i}{V} \quad (1)$$

166 I is the incident photon flow (kJ/s), Δt_i is the time interval (s) and V is the volume of the
167 treated solution (L).

168 Preliminary tests were performed to study the DPH adsorption onto the catalyst surface.
169 Different DPH concentrations (0, 12.5, 25, 50, 75 and 100 mg/L) were prepared with 0.4
170 g TiO₂/L, at natural pH (6.2), constant stirring and temperature (25°C ± 0.5) under dark
171 conditions. A two-parameter Langmuir isotherm model was tested in the fitting of
172 adsorption data (Eq. 2)

$$173 \quad q_e = \frac{q_m K_a C_e}{1 + K_a C_e} \quad (2)$$

174 q_e (mol/g) is the DPH amount adsorbed on the catalyst, C_e (mg/L) is the DPH
175 concentration in solution after adsorption, K_a is the Langmuir adsorption equilibrium
176 constant and q_m represents the maximum monolayer adsorption capacity. In our case, the
177 obtained values for K_a and q_m were 0.017 L/mol and 0.048 mol/g, respectively. These
178 low values of K_a and q_m show that adsorption does not play an important role.

179 To evaluate the temperature influence, 1 L of DPH solution with a concentration of 200
180 mg/L was placed in the stirred tank and heated at 20, 40, 60 and 80 °C. Degradation and/or
181 mineralization were not observed at any tested temperature.

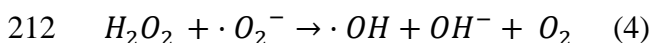
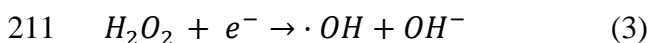
182 DPH degradation by photolysis was studied and experiments were carried out with 50
183 mg/L of DPH in the different reactors without catalyst. The influence of photolysis on
184 DPH degradation and mineralization is low in Solarbox (60 min, Q_{acc} = 3.5 kJ/L between

185 300-410 nm), CPC (60 min, $Q_{acc} = 2.28$ kJ/L between 315-400 nm) and BLB (60 min,
186 $Q_{acc} = 2.79$ kJ/L between 300-410 nm), the results were 2.5, 1.4 and 4.7% of DPH
187 degradation, respectively. Only UVC light (60 min, $Q_{acc} = 7.76$ kJ/L at 254 nm), achieving
188 32.5% of DPH removal in 60 min, is powerful enough to break the DPH bonds, because
189 UVC covers the range of light absorption of DPH (λ_{max} at 220 nm). Figure 1 summarizes
190 the obtained results. Moreover, photolysis did not promote relevant mineralization (4.5%
191 for BLB).

192 3.1. SB reactor

193 In SB, DPH elimination was (60 min, $Q_{acc} = 3.5$ kJ/L between 300-410 nm): 35.7% (for
194 0.4 g/L TiO_2), 27.0% (for 0.1 g/L TiO_2) and 15.8% (for 0.05 g/L TiO_2). TOC removal is
195 low and catalyst concentration does not significantly influence. Catalyst load can improve
196 DPH conversion. However, catalyst settling was observed for concentrations higher than
197 0.4 g/L TiO_2 in SB, decreasing the reaction rate by radiation scattering and catalyst losses.
198 The optimal loading depends on the photoreactor geometry and operation conditions [18
199 19].

200 The effect of H_2O_2 addition was evaluated, with 0.4 g/L of catalyst and 50 mg/L DPH, in
201 SB, BLB, UVC and CPC reactors. In SB, BLB and UVC three amounts of H_2O_2 (15, 75
202 or 150 mg/L) were added directly in the feeding tank. In CPC only 150 mg/L of H_2O_2
203 were used. In SB the highest degradation of DPH was obtained with 150 mg/L of H_2O_2
204 (62.6%). The joint presence of UV, H_2O_2 and TiO_2 improves DPH degradation. Several
205 articles have also reviewed that the addition of external oxidants such as hydrogen
206 peroxide, in this case, during the photocatalytic process can improve the degradation of
207 the organic matter when they are added in suitable dose [32,33]. H_2O_2 is considered to
208 have two functions in the photocatalytic oxidation. It accepts a photogenerated electron
209 from the conduction band of the semiconductor to form $\cdot OH$ radicals (Reaction 3). In
210 addition, it forms $\cdot OH$ radicals according to reaction 4 [34,35].



213 Moreover, as reported in different articles and pointed out in reaction 3, H_2O_2 is an
214 electron acceptor having a high activity and efficiency in this role than oxygen for the
215 titania conduction-band electrons [36,37]. However, mineralization levels in SB were

216 low: 9.0%, 9.8%, 10.7% and 16.3% TOC conversion for 0, 15, 75 or 150 mg/L of H₂O₂,
217 respectively. Figure 2 shows the results of DPH conversion and mineralization vs. the
218 accumulated energy (Q_{acc}, kJ/L) between 300-410 nm for different H₂O₂ concentrations.

219 **3.2. CPC reactor**

220 Figure 3 shows the obtained results of DPH conversion and mineralization vs. the
221 accumulated energy (Q_{acc}, kJ/L) in CPCs.

222 As commented in the section 3.1 and for the same reasons, the addition of hydrogen
223 peroxide improves the DPH degradation, as seen in Fig. 3 (360 min, Q_{acc} = 36 kJ/L
224 between 315-400 nm, 0.4 g/L TiO₂): 49.2% (without H₂O₂) and 69.5% (150 mg/L H₂O₂).
225 However, the TOC removal rate (11.2% without H₂O₂ and 13.7% with H₂O₂) has not
226 significant improvement. For comparison with the other experimental devices, the DPH
227 degradation, at 60 min of irradiation, was 8.7% (without H₂O₂) and 53.8% (with 150 mg/L
228 H₂O₂), while the TOC conversion was 5.6% and 6.7%, without H₂O₂ or with 150 mg/L
229 H₂O₂, respectively.

230 **3.3. BLB reactor**

231 Figure 4 shows the results of DPH conversion and mineralization vs. the accumulated
232 energy (Q_{acc}, kJ/L) for different H₂O₂ concentrations, in BLB reactor.

233 DPH elimination was (60 min, Q_{acc} = 2.79 kJ/L between 300-410 nm, 0.4 g/L TiO₂):
234 44.8% (without H₂O₂), 49.0% (15 mg/L H₂O₂), 55.6% (75 mg/L H₂O₂) and 64.9% (150
235 mg/L H₂O₂). The obtained results show that with 15 mg/L of H₂O₂ the DPH elimination
236 is not much higher, as it happens in SB. In BLB reactor only 4.2% more of degradation
237 was achieved with 15 mg/L H₂O₂. In the presence of high dose of hydrogen peroxide (150
238 mg/L H₂O₂) this degradation increases. However, the degradation values do not increase
239 more than 50% in BLB, SB and CPC, due to absorption wavelength (254 nm) of hydrogen
240 peroxide, as commented in section 3.4. As in the other tested experimental devices,
241 peroxide acts as additional source of hydroxyl radicals improving the overall efficiency,
242 as commented in section 3.1. Mineralization levels in this system were low too: 8.1%,
243 9.2%, 10.0% and 17.3 % with 0, 15, 75 and 150 mg/L of H₂O₂, respectively.

244 **3.4. UVC reactor**

245 In UVC reactor (Fig. 5), DPH elimination was (60 min, $Q_{acc} = 7.76$ kJ/L at 254 nm, 0.4
246 g/LTiO₂): 32.5% (without H₂O₂), 55.7% (15 mg/L H₂O₂), 79.7% (75 mg/L H₂O₂) and
247 100.0% (150 mg/L H₂O₂). As observed in the results in the presence with hydrogen
248 peroxide the degradation of DPH increases a 23.2% with minimum dose (15 mg/L H₂O₂).
249 Moreover, total DPH degradation was reached when 150 mg/L of H₂O₂ were employed.
250 Thus, in this reactor is observed much better the effect of hydrogen peroxide addition,
251 because the lamps emit at 254 nm and H₂O₂ absorbs at this wavelength. Again, the joint
252 presence of UV, H₂O₂ and TiO₂ improves DPH degradation. Moreover, not only
253 UV/TiO₂/H₂O₂ process acts, but also UV/H₂O₂ was deeding, which amplifies the effects
254 of the hydrogen peroxide manifested by reactions 3 and 4 in section 3.1. Mineralization
255 levels (without H₂O₂ or with 15 mg/L H₂O₂) were low too, but using 75 mg/L and 150
256 mg/L of H₂O₂ were achieved higher levels than for other conditions and reactor. TOC
257 conversion was 8.7% (without H₂O₂), 10.6% (with 15 mg/L H₂O₂), 23.3% (with 75 mg/L
258 H₂O₂) and 28.6% (with 150 mg/L H₂O₂).

259 **3.5. Energetic comparison of photocatalytic process in SB, BLB, UVC and CPC** 260 **reactors**

261 As beforehand observed, DPH removal and mineralization was evaluated in four different
262 experimental devices: a solar CPC pilot plant reactor, a solar simulator reactor (SB), a
263 three black light lamps based reactor (BLB) and a three UVC lamps based reactor. For
264 comparison, the selected experimental conditions were the same in all devices, differing
265 only in the geometry of the reactors and wavelength and radiation power. Energetic
266 comparisons were performed to evaluate the efficiencies (in DPH removal) referred to
267 the lamp power or referred to the energy associated to the wavelength range where TiO₂
268 absorbs (380-400 nm). The total efficiency for an experiment was calculated in each
269 device considering concentration (ppm/kWh) (Eq.3) or the total treated volume
270 (mg/kWh) (Eq.4). To determine kWh referred to the lamp power it was used the nominal
271 power of each lamp multiplied by the hours of experiment. The lamp power was 0.024
272 kWh for BLB and UVC reactors and 1 kWh for SB. The energy (kWh) associated to the
273 wavelength range where TiO₂ absorbs was determined by using actinometries in each
274 reactor. To assess the total cost for an experiment the inverse values of efficiency were
275 multiplied by the medium value of the electricity cost in Spain (0.13 €/kWh). Efficiency
276 and cost were evaluated for both DPH conversion and TOC removal at 60 minutes, as
277 Table 1 shows. Of course, for the evaluation of the global efficiency or global costs,

278 other parameters have to be considered such cost of installations, reactivities analysis, and
279 so one [38,39]. Here, only efficiencies referred to energy source were considered for a
280 quick and first approximation to the problem.

$$281 \frac{(ppm_{initial} - ppm_{final})}{kWh} \quad (5)$$

282

$$283 \frac{(ppm_{initial} - ppm_{final})}{kWh} \times Volume \quad (6)$$

284 In terms of lamp efficiency without H₂O₂, BLB presents the best results in all cases,
285 followed by UVC with similar results (see Table 1). It can also be observed that the use
286 of hydrogen peroxide improves the efficiency in all cases (two times in the case of BLB
287 and SB and four times in the case of UVC), probably due to the photolysis of H₂O₂ itself
288 and the generation of more hydroxyl radicals. With H₂O₂, UVC device shows the best
289 results. SB presents the worse results, due to the use of a lamp with 1kW power whereas
290 that UVC and BLB use lamps with 24 W power. The reasons for the observed differences
291 in DPH abatement can be related, obviously, to the geometry of devices and the radiation
292 used. The influence of radiation source is especially clear in the case of UVC that
293 becomes the best device when H₂O₂ is added to the reaction medium. This fact is due to
294 the photolysis of hydrogen peroxide favored in the UVC range (as commented before),
295 increasing the amount of hydroxyl radicals present in the medium and favoring the DPH
296 degradation. In addition, the geometry of the reactor used in UVC and BLB favors the
297 light improvement because lamps are located at the center of the cylindrical reactor. All
298 these reasons can explain that UVC and BLB offer best results than SB in DPH
299 abatement.

300 Other parameter interesting to evaluate is the efficiency referred to the range of absorption
301 for TiO₂, that is 380-400 nm. The energy corresponding to this interval has been
302 calculated from the radiation entering the photoreactors evaluated by actinometries, as
303 explained in section 2. In this case, the efficiency for UVC lamp cannot be calculated,
304 because UVC does not emit at 380-400 nm and the effect of TiO₂ is minimal. For similar
305 reasons, the experiments with hydrogen peroxide were not considered because the extra
306 hydroxyl radicals generated from H₂O₂ are produced out of the wavelength range
307 considered (380-400 nm). For the rest of tested devices, as observed in Table 1, it is

308 difficult to establish a general trend. When ppm reduction is considered, BLB and SB
309 present similar efficiencies and higher than CPC probably because the percentage of
310 radiation entering the photoreactor in the considered range (380-400 nm) is higher for
311 BLB and SB. However, if the reaction volume is taken into account and, therefore, the
312 efficiency is calculated with respect to the treated mg, the device showing clearly the best
313 results is BLB. This fact points out the importance of scaling when efficiencies are
314 considered, that means treated volume plays an important role when the efficiency of a
315 process is evaluated. The efficiency of the CPC is a further example in this sense, since,
316 taking into account the total volume treated, its efficiency in demineralization (mg
317 TOC/kWh) is lower than that obtained for BLB but even slightly higher than that obtained
318 for SB (14889, 21141 and 12222 for CPC, BLB and SB, respectively). Thus, the volume
319 treated in CPCs is large than in the other devices and this fact can imply an effect of
320 scaling up with the showed improvement of efficiency.

321 A draft economical comparison was performed to evaluate the costs for DPH removing
322 in each experimental device. As a first approximation, only the costs related to the
323 radiation source were considered, because these costs can highlight the importance of
324 well choosing the radiation source in carrying out an AOP. Obviously, solar natural
325 radiation based reactors (CPC) do not present costs in terms of electricity of lamps. When
326 all the power of the lamps is considered and H₂O₂ is not used, BLB device shows the
327 lowest costs and UVC shows slightly higher costs, although considering the efficiency in
328 TOC decrease, the costs are practically the same (see Table 1). The great difference
329 obviously appears when estimating the costs for SB that are much higher due to the power
330 difference of the lamps used, 1kW for SB and 24 W for BLB and UVC. When H₂O₂ is
331 used, things change and UVC happens to be the cheapest device with costs that are
332 practically half of those corresponding to BLB. SB remains the most expensive for the
333 reasons noted above (1kW of lamp power versus 24W of the other two). The change in
334 trend with hydrogen peroxide can also be explained by that already mentioned above,
335 when discussing the efficiencies, related to the increase of the photolysis of hydrogen
336 peroxide by the use of UVC radiation, favoring the generation of more hydroxyl radicals,
337 with the consequent increase of efficiency and costs reduction from an energetic point of
338 view.

339 When only the energy consumption in range between 380-400 nm is considered, UVC
340 and CPC are not included for the reasons explained before. Thus, the comparison between

341 BLB and SB shows that costs are similar, as observed in Table 1. The large differences
342 observed, when the entire power lamp was considered, disappear because in this case only
343 the radiation useful for titania absorption is considered.

344 Concerning the reaction kinetics, kinetic constants were obtained from the graphics \ln
345 $[DPH]/[DPH_0]$ vs accumulated energy (kJ) or vs irradiation time, at 60 min of irradiation
346 for all the cases. For the calculation of kinetic constants, the accumulated energy includes
347 the treated volume and, for this reason, the units are kJ. The accumulated energy was used
348 because radiation plays an important role in photocatalytic processes, influencing in a
349 decisive manner on the reaction rate. Thus, if only time is considered and the radiation
350 entering the reactors is omitted, we can arrive to a misinterpretation of the results. The
351 accumulated energy is the energy entering the photoreactor during all the experiment time
352 and was measured by actinometries, as explained, in section 2, except in the case of CPC
353 where radiation was measured by radiometers. The catalyst concentration was 0.4 g/L in
354 all the cases.

355 As shown in Table 1, when time fittings are considered (without H_2O_2), CPC shows the
356 low kinetic constant (h^{-1}) and BLB the best ones; however, UVC and SB present results
357 very close to BLB. When hydrogen peroxide was added, UVC gives the best results and
358 BLB, SB and CPC show similar results. The best results for UVC can be again related to
359 the photolysis of hydrogen peroxide by the UVC light and the increase of hydroxyl
360 radicals in the reaction medium, increasing the reaction rate.

361 If kinetics is referred to accumulated radiation instead time, the kinetic constants (kJ^{-1})
362 show the highest values for SB and BLB (0.122 and 0.107, respectively, see Table 1).
363 UVC shows a value four times lower (0.025) and CPC gives the poor value (0.008). This
364 behavior can be expected from the data observed in Figures 2-5, where CPC needs highest
365 amount of radiation to obtain conversion similar to that obtained for the other devices.
366 When hydrogen peroxide is added to reaction medium, UVC presents the highest value
367 for the kinetic constant ($0.493 kJ^{-1}$). This behavior is the same observed for all the tested
368 parameters, already commented, and is related to the increase of hydroxyl radicals due to
369 the photolysis of H_2O_2 in the UVC range. In this case, SB ($0.282 kJ^{-1}$) shows results
370 slightly better than BLB ($0.188 kJ^{-1}$), being again CPC giving the low kinetic constant
371 ($0.021 kJ^{-1}$).

372 All the results commented in this section point out the influence of radiation and reactor
373 geometry on the reaction rate and consequently on the pollutant degradation. The
374 importance of taking into account radiation instead of time, when calculating the kinetic
375 constants, has also been shown. Finally, it is also clear that, when comparisons are made,
376 it is necessary to indicate clearly how they have been done. Thus, it has been shown that
377 it is not the same to evaluate the efficiency in the degradation of the pollutant per kWh
378 taking into account the absolute amount degraded (ppm) or also taking into account the
379 treated reaction volume (mg). Moreover, it is necessary to specify clearly how the
380 radiation efficiency is calculated: radiation emitted by the lamp, radiation that can absorb
381 the catalyst, etc.

382 **3.6. Toxicity, intermediates and degradation pathways**

383 Regarding to hazardousness of treated solutions, toxicity (*vibrio fischeri*) was assessed for
384 the different experimental conditions in all devices. This includes experiments without
385 H₂O₂ and experiments with H₂O₂ (15, 75, 150 mg/L). The *vibrio fischeri* test indicated that
386 DPH was initially non-toxic. However, after performing the experiments on the different
387 experimental devices, the test was repeated to verify that the intermediates that could be
388 generated were also non-toxic. In fact, it was verified in all cases that the tests of *vibrio*
389 *fischeri* indicate that final solutions were non-toxic.

390 Intermediates identification was performed with samples taken at 60 min of irradiation in
391 all the devices, with all experimental conditions. The intermediates identified are shown
392 in Table 2. These intermediates were the same under the different radiation sources and
393 different experimental devices tested and no significant difference was observed when
394 the concentrations of H₂O₂ were varied.

395 According to the intermediates found and their proposed structures, pathways can be
396 proposed (Figure 6).

397 The photocatalytic process lets to the formation of *m/z* 104, *m/z* 272 and *m/z* 274 (DPH
398 104, DPH-272 and DPH-274). Formation of DPH-104 could be by cleavage of DPH-256
399 and subsequently hydroxylation of two carbons and oxidation of one of them. Meanwhile,
400 DPH-272 could be formed from DPH-256 by the hydroxylation of the molecule.
401 Furthermore, due to OH· generation, it is logical to expect the addition of OH· on the
402 aromatic ring and to open the aromatic ring leading to the formation of DPH-274.

403 Moreover, the hydroxylation form of DPH-274 could be attacked by $\text{OH}\cdot$ forming a
404 compound (DPH-290). In the same way, when the hydrogen peroxide was added DPH-
405 306, DPH-322 and DPH-338 were formed. This is due to the formation of more $\text{OH}\cdot$
406 when there is more addition of peroxide. Thus, it is logical that these compounds are
407 formed [40]. In addition, the low mineralization observed in all the cases agrees the
408 proposed reaction pathway. Summarizing, from the reaction intermediates that could be
409 detected, it appears that the oxidation processes occur mainly through the hydroxyl
410 radicals, as indicated in Figure 6 and, therefore, it seemed that the other mechanisms had
411 a secondary role. It also seems very likely that molecular oxygen will act as an electron
412 acceptor by giving the radical superoxide anion ($\cdot\text{O}_2^-$) [34], but in turn it reacts rapidly
413 with hydrogen peroxide to give hydroxyl radicals (see reaction 4 in section 3.1)
414 reinforcing the role of hydroxyl radicals.

415 **4. CONCLUSIONS**

416 The four devices tested (UVC, BLB, SB and CPC) are useful for DPH degradation by
417 TiO_2 photocatalysis, obtaining the best results in BLB (44.8% DPH degradation).
418 However, mineralization is very low in all the cases. In the case of UVC system, the DPH
419 and TOC removal are due mainly to photolysis. In this way, results improve when H_2O_2
420 was added and the best results were obtained in UVC with 100% of DPH degradation,
421 being the mineralization 28.6%. This improvement can be explained by the photolysis of
422 hydrogen peroxide in UVC system, increasing the generation of hydroxyl radicals and,
423 therefore, the reaction rate. Considering the efficiency referred to lamp power, BLB
424 (without H_2O_2) and UVC (with H_2O_2) show the highest efficiencies (mg DPH/kWh and
425 ppm DPH/kWh) in the photocatalytic treatment of DPH. This behavior agrees with the
426 observation that UVC gives the highest kinetic (kJ^{-1}) constant and the highest conversion
427 because the power of lamp promotes also the photolysis of H_2O_2 increasing the presence
428 of hydroxyl radicals and, consequently, the reaction rate. Concerning the costs ($\text{€}/\text{mg}$
429 DPH or $\text{€}/\text{ppm DPH}$) the observed trends are the same, SB presents the worst results
430 respect to the lamp efficiency due to the highest lamp power (1000 W for SB and 24 W
431 for BLB and UVC). In terms of efficiency in the absorption range of TiO_2 (380-400
432 nm), BLB presents the best results in DPH degradation, followed by SB and CPC.
433 Toxicity studies pointed out that DPH can be considered non-toxic and neither its
434 intermediates. The intermediates obtained in the photocatalytic treatment of DPH show,
435 on the one hand, that the breakdown of the DPH molecule and subsequent hydroxylation

436 of the molecule proceeds; while, on the other hand, they also indicate that hydroxylations
437 occur on the DPH molecule because of the hydroxyl radicals generated.

438 **Acknowledgments**

439 The authors thank the Ministry of Science and Innovation of Spain (projects CTQ2014-
440 52607-R) and AGAUR-Generalitat de Catalunya (project 20145GR245) for funding this
441 research.

442 **References**

443 [1] N. Miranda-García, M. Ignacio Maldonado, J.M. Coronado, S. Malato, Degradation
444 study of 15 emerging contaminants at low concentration by immobilized TiO₂ in a pilot
445 plant, *Catal. Today* 151 (2010) 107-113.

446 [2] European Commission Joint Research Centre, Directive 2013/39/EU of the European
447 Parliament and of the Council amending Directives 2000/60/EC and 2008/105/EC as
448 regards priority substances in the field of water policy. Part I. EUR 2011/429 EN, *Eur.*
449 *Chem. Bur. Part II* (2013) 226/1–226/17.

450 [3] J. Munthe, E. Brorström-Lundén, M. Rahmberg, L. Posthuma, R. Altenburguer, W.
451 Brack, D. Bunke, G. Engelen, B.M. Gawlick, J. Van Gils, D., T., LópezHerráez Rydberg,
452 J. Slobodnik, A. Van Wezel, An expanded conceptual framework for solution-focused
453 management of chemical pollution in European waters, *Environ. Sci. Eur.* Vol. 29, Issue
454 1, Article number 13 (2017).

455 [4] D.J. Lapwortha, N. Baranb, M.E. Stuarda, R.S. Warda, Review emerging organic
456 contaminants in groundwater: a review of sources, fate and occurrence, *Environ. Pollut.*
457 163 (2012) 287-303.

458 [5] S. Alonso, M. Catalá, R. Maroto, Pollution by psychoactive pharmaceuticals in the
459 Rivers of Madrid metropolitan area (Spain), *Environ. Int.* 36 (2010) 195–201.

460 [6] N. Miranda, S. Miranda, I.M. Maldonado, S. Malato, B. Sánchez, Regeneration
461 approaches for TiO₂ immobilized photocatalyst used in the elimination of emerging
462 contaminants in water, *Catal. Today* 230 (2014) 27-34.

- 463 [7] S.D. Richardson, *Environmental Mass Spectrometry: Emerging Contaminants and*
464 *Current Issues*, *Anal. Chem.* 80 (12) (2008) 4373-4402.
- 465 [8] B. Kasprzyk-Hordern, R.M. Dinsdale, A.J. Guwy, The occurrence of pharmaceuticals,
466 personal care products, endocrine disruptors and illicit drugs in surface water in South
467 Wales, UK, *Water Res.* 42 (13) (2008) 3498-3518.
- 468 [9] A. De Luca, R.F. Dantas, S. Esplugas, Assessment of iron chelates efficiency for
469 photo-Fenton at neutral pH, *Water Res.* 61 (2014) 232-242.
- 470 [10] Z.Yimeng, C.Wenhai, X.Ting, Y.Daqiag, Y.Bin, L.Pan, A.Na, Impact of pre-
471 oxidation using H₂O₂ and ultraviolet/H₂O₂ on disinfection byproducts generated from
472 chlor(am)ination of chloroamphenicol, *Chem. Eng. Journal* 317 (2017) 112-118.
- 473 [11] B.I. Escher, R. Baumgartner, M. Koller, K. Treller, J. Linert, C.D. McCardell,
474 *Environmental toxicology and risk assessment of pharmaceuticals from hospital*
475 *wastewater*, *Water Res.* 45 (2011) 75-92.
- 476 [12] D.G. Joakim Larrson, C. De Pedro, N. Paxeus, Effluent from drug manufactures
477 contains extremely high levels of pharmaceuticals, *Journal Hazard. Mater.* 148 (2007)
478 751-755.
- 479 [13] A. Moraes, A. Schwarz, H. Spinosa, Maternal exposure to diphenhydramine during
480 the fetal period in rats: Effects on physical and neurobehavioral development and on
481 neurochemical parameters, *Neurotox. and Teratol.* 26 (2004) 681-692.
- 482 [14] V. Roos, L.Gunnarsson, J.Fick, Prioritising pharmaceuticals for environmental risk
483 assessment: Towards adequate and feasible first-tier selection, *Sci. Total Environ.* 421-
484 422 (2012) 102-110.
- 485 [15] B. Ning, N. Graham, Y.P. Zhang, M. Nakonechny, M.G. El Din, Degradation of
486 endocrine disrupting chemicals by ozone/AOPS, *Ozone: Sci. Eng.* 29 (2007) 153-176.
- 487 [16] N. De la Cruz, J. Giménez, S. Esplugas, D. Granjean, L.F. De Alencastro, C.
488 Pulgarín, Degradation of 32 emergent contaminants by UV and neutral photo-fenton in
489 domestic wastewater effluent previously treated by activated sludge, *Water Res.* 45 (6)
490 (2012) 1947-1957.

- 491 [17] I. Sirés, E., Brillas, Remediation of water pollution caused by pharmaceutical
492 residues based on electrochemical separation and degradation technologies: a
493 review, *Environ. Int.* 40 (2012) 212–29.
- 494 [18] R.A.R. Monteiro, S.M. Miranda, V.J.P. Vilar, L.L. Pastrana-Martínez, P.B.
495 Tavares, R.A.R. Boaventura, J.L. Faria, E. Pinto, A.M.T. Silva, N-modified TiO₂
496 photocatalytic activity towards diphenhydramine degradation and *Escherichia coli*
497 inactivation in aqueous solutions, *App. Catal. B: Environ.* 162 (2015) 66-74.
- 498 [19] L.M. Pastrana-Martínez, J.L. Faria, J.M., Doña-Rodríguez, C. Fernández-
499 Rodríguez, A.M.T. Silva, Degradation of diphenhydramine pharmaceutical in aqueous
500 solutions by using two highly active TiO₂ photocatalyst: Operating parameters and
501 photocatalytic mechanism, *Appl. Catal. B: Environ.* 113-114 (2012)221-227.
- 502 [20] S. Malato, P. Fernández-Ibáñez, M. I. Maldonado, I. Oller, M. I. Polo-López, Solar
503 Photocatalytic Pilot Plants: Commercially Available Reactors, in: Pierre Pichat (Eds.),
504 Photocatalysis and Water Purification, Wiley-VCH, Weinheim-Germany (2013) 377-
505 397.
- 506 [21] D. G. Joakim Larsson, C. De Pedro, N. Paxeus, Effluent from drug manufactures
507 contains extremely high levels of pharmaceuticals, *Journal Hazard. Mater.* 148 (2007)
508 751-755.
- 509 [22] N. De la Cruz, V. Romero, R.F. Dantas, P. Marco, B. Bayarri, J. Giménez, S.
510 Esplugas, O-Nitrobenzaldehydeactinometry in the presence of suspended TiO₂ for
511 photocatalytic reactors, *Catal. Today* 209 (2013) 209-214.
- 512 [23] N. De la Cruz, R.F. Dantas, J. Giménez, S. Esplugas, Photolysis and TiO₂
513 photocatalysis of the pharmaceutical propranolol: Solar and artificial light”, *Appl. Catal.*
514 *B-Environ.* 130-131 (2013) 249-256.
- 515 [24] V. Romero, F. Méndez-Arriaga, P. Marco, J. Giménez, S. Esplugas, “Comparing the
516 photocatalytic oxidation of Metoprolol in a solarbox and a solar pilot plant reactor”,
517 *Chem. Eng. J.* 254 (2014) 17-29.
- 518 [25] V. Romero, “Degradation of metoprolol by means of advanced oxidation processes”,
519 Doctoral Thesis, University of Barcelona (2015). <http://hdl.handle.net/2445/65724>

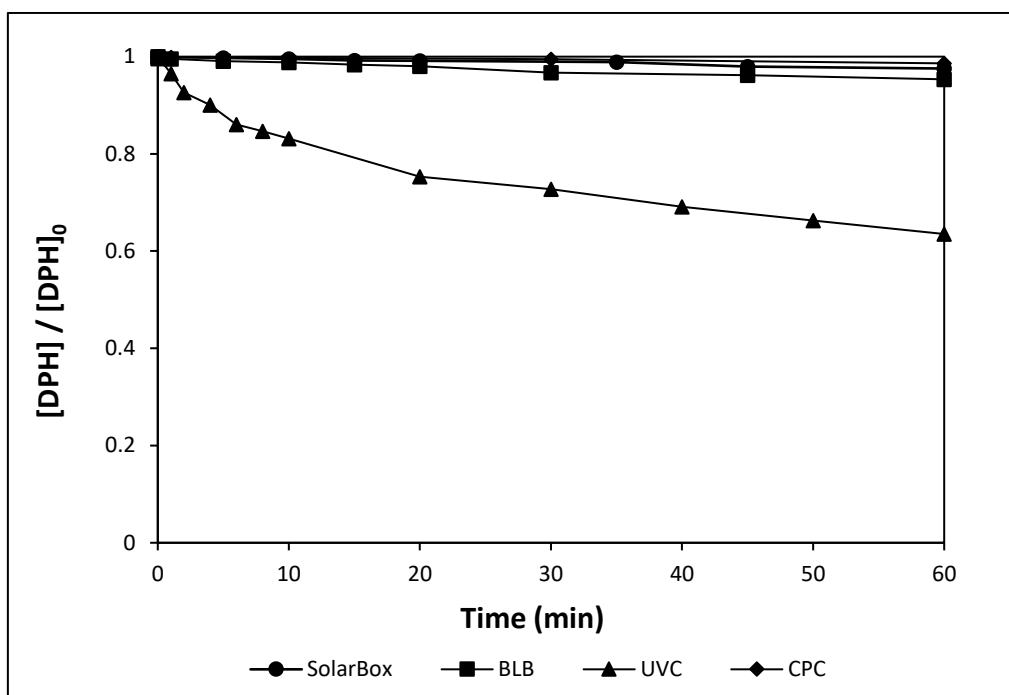
- 520 [26] H.J. Kuhn, S.E. Braslavsky, R. Schmidt, Chemical actinometry (IUPAC Technical
521 Report), Pure. Appl. Chem. 76 (2004) 2105-2146.
- 522 [27] V. Romero, D. De la Cruz, R.F. Dantas, P. Marco, J. Giménez, S. Esplugas,
523 Photocatalytic treatment of metoprolol and propranolol, Catal. Today 161 (2011) 115-
524 120.
- 525 [28] V. Romero, P. Marco, J. Giménez, S. Esplugas, Adsorption and Photocatalytic
526 Decomposition of the β -Blocker Metoprolol in Aqueous Titanium Dioxide Suspensions:
527 Kinetics, Intermediates, and Degradation Pathways, Int. Journal Photoenerg. (2013) 1-
528 10.
- 529 [29] V. Romero, O. González, B. Bayarri, P. Marco, J. Giménez, S. Esplugas,
530 Performance of different advanced oxidation technologies for the abatement of the beta-
531 blocker metoprolol, Catal. Today 240 (2015) 86-92.
- 532 [30] V. Romero, O. González, B. Bayarri, P. Marco, J. Giménez, S. Esplugas,
533 Degradation of Metoprolol by photo-Fenton: Comparison of different photoreactors
534 performance, Chem. Eng. Journal 283 (2016) 639-648
- 535 [31] P. Fernández, J. Blanco, C. Sichel, S. Malato, Water disinfection by solar
536 photocatalysis using compound parabolic collectors, Catal. Today 101 (2005) 345-352.
- 537 [32] F.J. Beltrán, F.J. Rivas, R. Montero-de-Espinosa, Catalytic ozonation of oxalic acid
538 in aqueous TiO₂ slurry reactor, Appl. Catal. B: Environ. 39 (2002) 221.
539
- 540 [33] S.G. De Moraes, R.S. Freire, N. Duran, Degradation and toxicity reduction of textile
541 effluent by combined photocatalytic and ozonation processes, Chemosphere 40 (2000)
542 369
- 543 [34] E.S., Elmolla, M. Chaudhuri, Photocatalytic degradation of amoxicillin, ampicillin
544 and cloxacillin antibiotics in aqueous solution using UV/TiO₂ and UV/H₂O₂/TiO₂
545 photocatalysis, Desalination 252 (2010) 46-52.
- 546 [35] M. Kositzi, A. Antoniadis, I. Poulios, I. Kiridis, S. Malato, Solar photocatalytic
547 treatment of simulated dyestuff effluents, Sol. Ener. 77 (2004) 591-600.

- 548 [36] Z. Wang, C.S. Hong, Effect of hydrogen peroxide, periodate and persulfate on
549 photocatalysis of 2-chlorobiphenyl in aqueous TiO₂ suspensions, *Water Res.* 33 (1999)
550 2031.
- 551 [37] J. Fernández, J. Kiwi, J. Baeza, J. Freer, C. Lizama, H.D. Mansilla, Orange II
552 photocatalysis on immobilized TiO₂ Effect of the pH and H₂O₂, *Appl. Catal. B: Environ.*
553 48 (2004) 205-211.
- 554
555 [38] J. Giménez, B. Bayarri, O. González, S. Malato, J. Peral, S. Esplugas, Advanced
556 Oxidation Processes at laboratory scale: Environmental and Economic Impacts, *Sustain.*
557 *Chem. Eng.* 3 (2015) 3188–3196.
- 558 [39] D. Haranaka Funai, F. Didier, J. Giménez, P. Marco, S. Esplugas, A. Machulek
559 Junior, Photocatalytic treatment of valproic acid sodium salt with TiO₂ in different
560 experimental devices: an economic and energetic comparison, *Chem. Eng. Journal* 327
561 (2017) 656–665.
- 562 [40] L.M. Pastrana-Martínez, N. Pereira, R. Lima, J.L. Faria, H. T. Gomez, A.M.T.,
563 Silva, Degradation of diphenhydramine by photo-Fenton using magnetically recoverable
564 iron oxide nanoparticles as catalyst, *Chem. Eng. Journal* 261 (2015) 45-52.

565

566

567



568

Figure 1. DPH degradation by photolysis in all experimental devices.

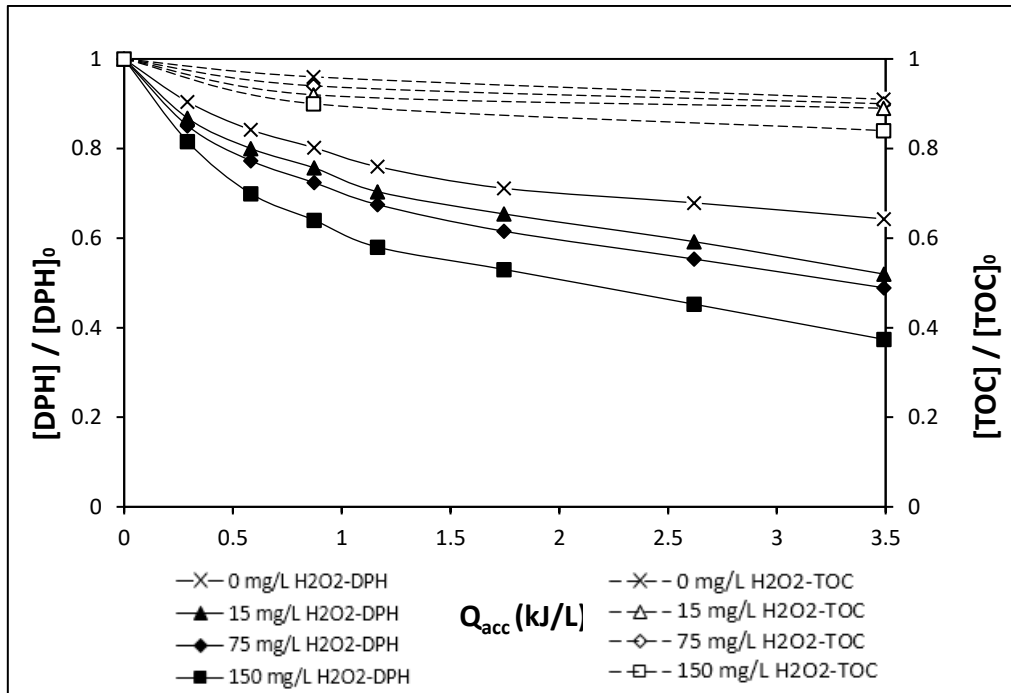
569

570

571

572

573



574

575

576

Figure 2. DPH conversion and TOC removal in SB reactor for different H_2O_2 concentrations at 60 min. $[TiO_2] = 0.4$ g/L

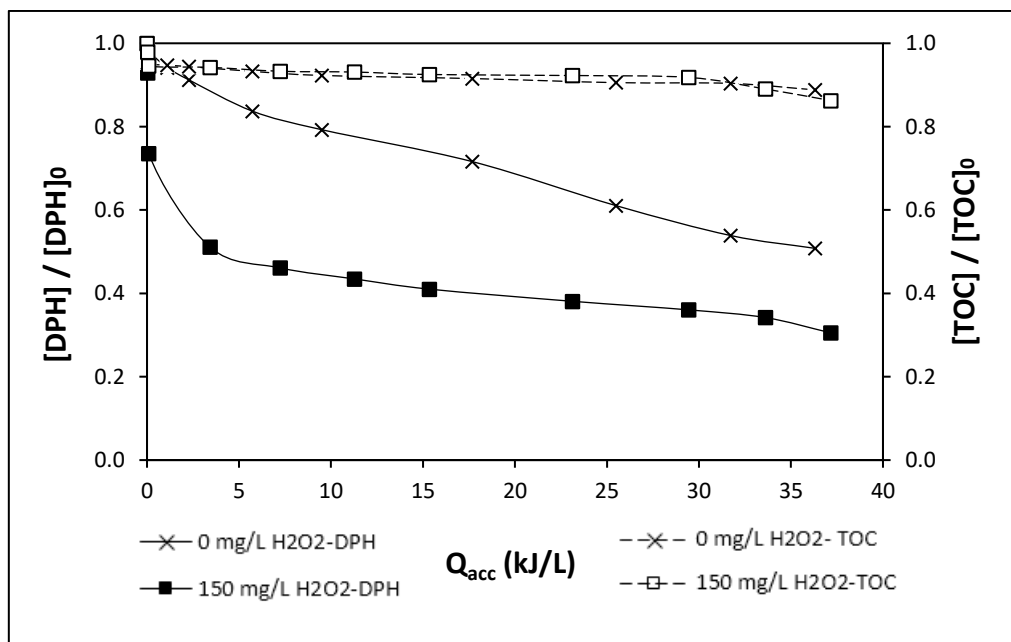
577

578

579

580

581



582

583

Figure 3. DPH conversion and TOC removal in CPC reactor at 360 min.

584

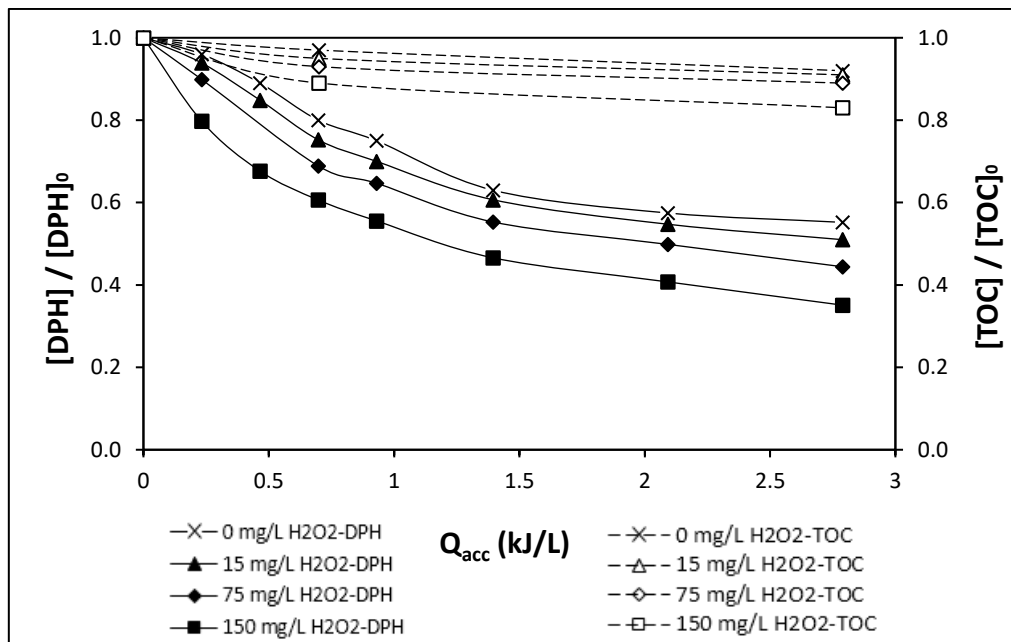
$[TiO_2] = 0.4$ g/L

585

586

587

588



589

590

Figure 4. DPH conversion and TOC removal in BLB reactor at 60 min.

591

$[TiO_2] = 0.4$ g/L

592

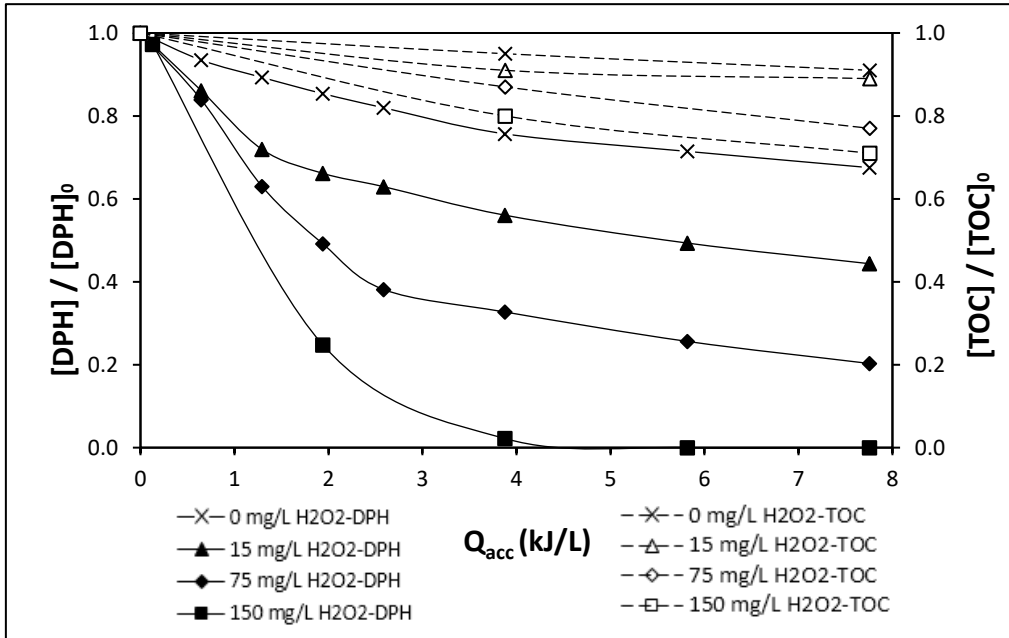
593

594

595

596

597



608

609 **Figure 5. DPH conversion and TOC removal in UVC reactor at 60 min.**

610

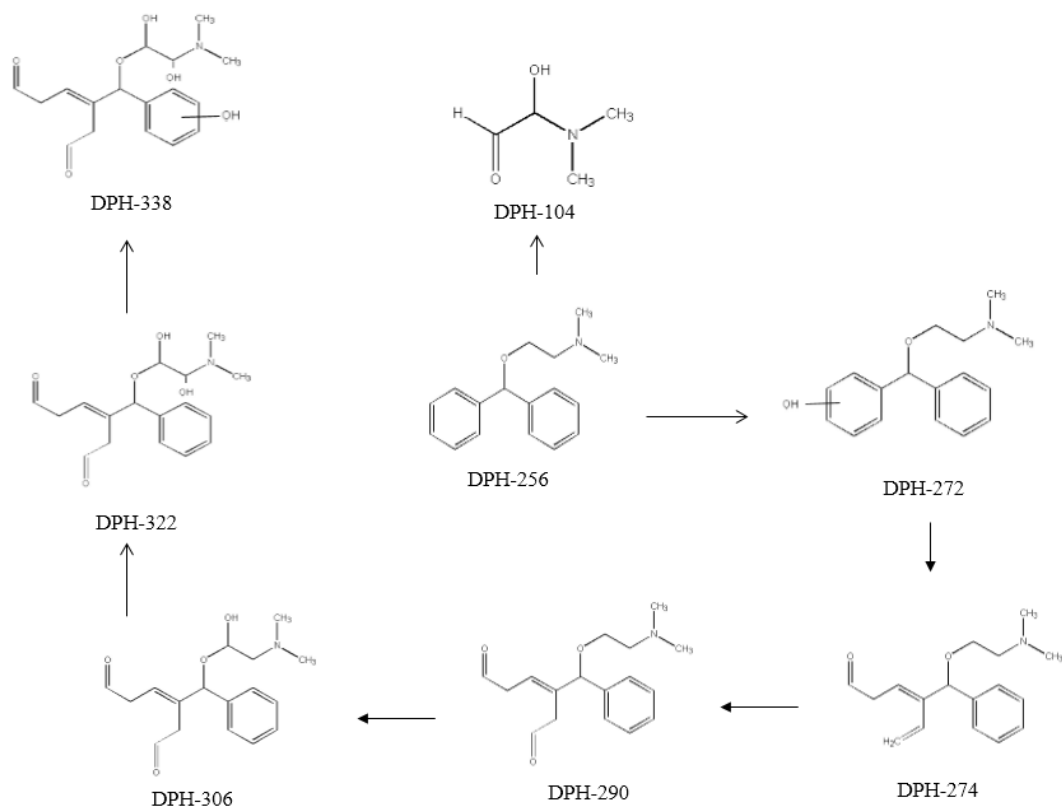
$[TiO_2] = 0.4 \text{ g/L}$

611

612

613

614



615

616 **Figure 6.** Proposed DPH degradation pathways for photocatalytic process.

617

618

619